Available online at www.sciencedirect.com
SCIENCE DIRECT®
Biomaterials 25 (2004) 4057–4064
Biomaterials
www.elsevier.com/locate/biomaterials

Effect of surface finish on the osseointegration of laser-treated titanium alloy implants

H.E. Götz[a], M. Müller[b], A. Emmel[c], U. Holzwarth[d], R.G. Erben[a], R. Stangl[b,*]

[a] Veterinary Faculty, Institute of Physiology, Physiological Chemistry and Animal Nutrition, Ludwig Maximilians University, Munich, Germany
[b] Trauma Surgery Division at the Friedrich Alexander University Hospital Department of Surgery, Erlangen/Nürnberg, Germany
[c] University of Applied Sciences, Amberg, Germany
[d] P. Brehm Co., Weisendorf, Germany

Received 23 July 2003; accepted 8 November 2003

Abstract

It was the purpose of this study to examine the osseointegration of laser-textured titanium alloy (Ti6Al4 V) implants with pore sizes of 100, 200, and 300 μm, specifically comparing 200-μm implants with polished and corundum-blasted surfaces in a rabbit transcortical model. Using a distal and proximal implantation site in the distal femoral cortex, each animal received all four different implants in both femora. The bone–implant interface and the newly formed bone tissue within the pores and in peri-implant bone tissue were examined 3, 6, and 12 weeks post-implantation by static and dynamic histomorphometry. Here we show that additional surface blasting of laser-textured Ti6Al4 V implants with 200-μm pores resulted in a profound improvement in osseointegration, 12 weeks postimplantation. Although lamellar bone formation was found in pores of all sizes, the amount of lamellar bone within pores was linearly related to pore size. In 100-μm pores, bone remodeling occurred with a pronounced time lag relative to larger pores. Implants with 300-μm pores showed a delayed osseointegration compared with 200-μm pores. We conclude that 200 μm may be the optimal pore size for laser-textured Ti6Al4 V implants, and that laser treating in combination with surface blasting may be a very interesting technology for the structuring of implant surfaces.

Keywords: Titanium alloy; Laser; Porosity; Histomorphometry; Osseointegration

1. Introduction

A stable anchoring is critical for long-term success of total hip arthroplasties, avoiding pain for the patient, functional impairment, and eventually revision of the implant. To achieve lasting stability of non-cemented implants, osseointegration of the implant is a prerequisite [1]. Osseointegration is defined as the direct connection from implant to living remodeling bone without any soft tissue component between implant and bone on the light microscopic level [2]. A rapid osseointegration is associated with improved secondary stability and, thus, with a favorable prognosis for long-term success of the implant [3,4]. To allow early fibrin adhesion, blood vessel growth and eventually new bone-formation, initial stability has to be achieved by reduction of micromotion [1,5,6]. If micromotion cannot be reduced to a minimum level, a fibrous tissue instead of a bony interface will result at the implant surface [2,7–9].

In order to reduce micromotion initially, and to improve osseointegration later on, many variants in surface geometry of the implant have been developed [10–12]. It is well known that surface geometry determines the interactions of proteins and cells with the implant surface [13,14], and that increased surface roughness is associated with better cell adherence, higher bone–implant contact (BIC), and improved biomechanical interaction [6,15–19].

It is evident that bone ingrowth into porous implant surfaces may result in improved osseointegration and mechanical stability by interlocking the surrounding bone tissue with the implant [20–22]. Implants with different pore sizes were investigated by Bobyn [23], who reported an optimum pore size of 100–400 μm. Several

*Corresponding author. Chirurgische Universitaetsklinik Erlangen, Abteilung fuer Unfallchirurgie, Krankenhausstrasse 12, 91054 Erlangen, Germany. Tel.: +49-9131-8533296; fax: +49-9131-8533300.
E-mail address: richard.stangl@web.de (R. Stangl).

0142-9612/$ - see front matter © 2003 Elsevier Ltd. All rights reserved.
doi:10.1016/j.biomaterials.2003.11.002

other studies have shown that there appears to be a minimum pore size of about 140–200 μm for viable osteons to arise [12,24,25]. Osteons in cortical bone and hemiosteons in cancellous bone are created by bone remodeling activities [26], replacing biomechanically inferior woven bone by lamellar bone, and removing microdamage that may have accumulated at the bone–implant interface [27]. Thus, remodeling of bone within pores is essential for long-term stability of the bone–implant interface.

To achieve a porous surface, implants usually have been manufactured as solid rods, and were then sintered with beads or fiber mesh due to the lack of a technology to homogeneously create open interconnecting structures in titanium alloys [28]. However, the sintering process can lead to brittleness and reduced fatigue strength [29]. Recent progress in laser technology has made it possible to produce novel implant surfaces by introducing pores of defined geometry into metal implants with high precision and efficiency [30]. In a previous study conducted in our laboratory, we examined the osseointegration of copper vapor laser-textured titanium alloy (Ti6Al4 V) implants with pore sizes of 25, 50, and 200 μm in a rabbit intramedullary model [31]. We found that implants with 50- and 200-μm pore sizes had the highest values for BIC among the laser-textured surfaces, and that bone remodeling within pores occurred only in the implants with 200-μm pores. However, all laser-textured implants were inferior to corundum-blasted (CB) control implants in terms of osseointegration, most likely due to the fact that the implant surface between the pores was smoothly polished in our previous investigation. Therefore, we sought to examine the osseointegration of laser-textured Ti6Al4 V implants with pore sizes of 100, 200, and 300 μm in the present investigation, specifically comparing 200-μm implants with polished and CB surfaces. We chose a rabbit transcortical model in this study in order to expand our model to situations with increased compression loading such as those found in noncemented endoprosthetic hip cups. Here we show that surface-blasted implants with 200-μm pores are superior to polished implants with any pore size in terms of osseointegration.

2. Materials and methods

2.1. Implants

Ti6Al4 V cylinders of 5.5 mm length and 3.5 mm diameter were used (Brehm, Weisendorf, Germany). Using a neodyme (Nd):YAG laser, pores of defined geometry were introduced into the surface of the polished, lathed implants by the ATZ-EVUS company (Vilseck, Germany), and by the University of Applied Sciences, Amberg, Germany. The laser generated a maximum power of up to 65 W. Nanosecond timing of each amplifier resonance point permitted firing of a predetermined number of pulses of up to 100 ns duration at high repetition rates (10 kHz). In this study, we used pore diameters of 100, 200, and 300 μm. Pore depth and pore diameter were identical. The pores were conical or cylindrical in shape and the distance between the pores was the same as pore diameter. The sharp edges of the pores were smoothed with fine sandpaper. Half of the implants with 200-μm pores were additionally blasted with 500–710 μm Al_2O_3 grit. Surface roughness was measured by non-contact surface profilometry (Mahr, Göttingen, Germany), and a mean inter-pore roughness of 7.25 μm (R_a) was achieved for blasted 200-μm implants. After surface treatment, the implants were cleaned ultrasonically, and sterilized industrially using gamma irradiation (28 kV).

2.2. Experimental animals and surgical procedures

All animal experiments were approved by the government authorities. Forty-five adult female New Zealand White rabbits with mature skeletons and an average body weight of 3.2 kg were used for this experiment. The animals were jointly housed in runs. Each animal received two implants in each femur. Thus, each rabbit received all 4 different implants. The implants were randomly assigned to the two different implantation sites.

The animals were anesthetized with an intramuscular injection of 25 mg/kg ketamine (Parke & Davis, Freiburg, Germany) and 5 mg/kg xylazine (Boehringer, Ingelheim, Germany). Anesthesia was maintained with intravenous injections of ketamine/xylazine. Immediately before the operation the rabbits received 0.4 ml benzyl penicillin (Tardomyocel®, Boehringer, Ingelheim, Germany). After shaving, depilation (Pilca med®, Schwarzkopf und Henkel, Düsseldorf, Germany), and desinfection (Betaisodona®, Mundipharma, Limburg, Germany) of the skin, the distal femur was exposed by a lateral incision. The incisions were infiltrated with 2% lidocaine (Hoechst, Frankfurt, Germany). Two holes (proximal and distal, 3.2 mm in diameter) were carefully drilled into the lateral cortical bone of the distal femur under generous irrigation with saline to reduce the heat generated by drilling. The implants were placed transcortically in the holes by press-fit insertion. Finally, the incision was closed in layers. At the end of the procedure, all animals received a subcutaneous injection of 0.1 mg/kg buprenorphine (Essex, München, Germany) as an analgesic. Subsequent analgesic therapy was performed with metamizole (Hoechst) administered via the drinking water (5 mg/l) over 2 days postsurgery.

Normal weight-bearing was permitted after the implantation. Most of the wounds healed without complications. Two animals died under anesthesia, and four rabbits had to be killed a few days after the operation because of patella luxation or weight loss. As markers for bone formation dynamics, 4 different fluorochromes (alizarine complexone 20 mg/kg body weight, xylenol orange 90 mg/kg, calcein green 10 mg/kg, oxytetracycline 30 mg/kg; ICN, Ohio, USA) were injected subcutaneously according to the regimen shown in Table 1. Groups of 11–15 animals each was killed by an intraperitoneal pentobarbital overdose 3, 6, and 12 weeks postsurgery.

2.3. Histology

At necropsy, the femora were removed, and trimmed with a saw under fluoroscopic control. With the implants in situ, these bone cylinders were then dehydrated in ascending alcohol solutions and embedded undecalcified in methylmethacrylate in cylindrical glass vials as described [32]. Proceeding from periosteal to endocortical, at least six consecutive sections of approximately 200 μm thickness were made with a precision band saw (Exakt, Norderstedt, Germany) from each specimen. Subsequently, the sections were ground to a final thickness of 20 μm with the help of the micro-grinding system (Exakt) as described [33]. The sections were initially left unstained for fluorochrome-based measurements. Thereafter, the sections were stained with toluidine blue for subsequent measurements of bone–implant contact.

2.4. Histomorphometry

2.4.1. Bone growth within pores and in peri-implant tissue

Measurements of fluorochrome-based histomorphometric parameters of bone formation within the pores and in the area within 0.5 mm from the implant surface were made using a Videoplan semiautomatic system (C. Zeiss, Jena, Germany) and a Zeiss Axioskop microscope with a drawing attachment in unstained sections. Measurements of peri-implant bone growth were performed only in the 12-week group. One section was analyzed per implant. The labeled perimeter (L.Pm/B.Pm) was defined as the percentage of fluorochrome-labeled bone perimeter for each fluorochrome label, and was measured at $\times 200$. The mineral apposition rate (MAR) between two adjacent fluorochrome labels was measured at $\times 200$, sampling each site showing both labels every 50 μm. Values for MAR were not corrected for obliquity of the plane of section. The bone formation rate (BFR/T.Ar) for the time interval between two fluorochrome labels was calculated by multiplying the arithmetic mean of the two individual values for labeled perimeter with the respective MAR. All bone formation rates were normalized to the pore area or to the peri-implant measuring area in order to account for differences in total area available for these measurements.

2.4.2. Bone–implant interface

Measurements of BIC were made with a semiautomatic system (Videoplan, C. Zeiss) and a Zeiss Axioskop microscope with a drawing attachment on one section stained with toluidine blue at $\times 100$. BIC was measured separately within the pores, and on the outer surface of the implant. Total BIC was calculated as the sum of within-pore BIC and surface BIC.

2.4.3. Bone quality within pores

Using the Videoplan semiautomatic system (C. Zeiss), the pore area, and the total and lamellar bone area within the pores were measured under polarized light on sections stained with toluidine blue at $\times 100$. From these primary data, the percentages of pore filling, and of lamellar and woven bone were calculated.

2.5. Statistical analysis

Statistical data analysis was performed using SPSS 11.0 (SPSS, Chicago, IL, USA). Initially, the data from all time points (3, 6, and 12 weeks) were analyzed using a three-way factorial analysis of variance (ANOVA) with the factors *implant surface* (100-, 200-, 300-μm pores, and blasted 200-μm pores), *implantation site* (distal, proximal), and *time postsurgery* (3, 6, 12 weeks). Three-way factorial ANOVA evaluated whether the above-mentioned factors had a statistically significant effect, and also determined whether there was a two-way interaction between the individual factors. Thus, this statistical technique allows telling whether two different factors mutually influence each other in a non-additive way.

Table 1
Fluorochrome labeling regimen

Time point	Postoperative day	Substance
3 weeks	10	Alizarine complexone
	15	Calcein green
	19	Xylenol orange
6 weeks	10	Alizarine complexone
	20	Calcein green
	30	Xylenol orange
	40	Oxytetracycline
12 weeks	15	Alizarine complexone
	31	Calcein green
	47	Xylenol orange
	63	Oxytetracycline

Subsequently, using only *implant surface* as variable, the combined data from each time point were analyzed by one-way ANOVA followed by Student–Neumann–Keuls multiple comparison test.

P values of less than 0.05 were considered significant for all statistical analyses. The data are presented as the mean ± SEM.

3. Results

3.1. Factorial ANOVA

Factorial ANOVA showed that the variables *implant surface* and *time postimplantation* had a significant effect on total and surface BIC, on pore filling, and on the amount of lamellar bone within pores (Table 2). The within-pore BIC was not influenced by the type of implant surface, but increased significantly with time (see below). The *implantation site* (proximal or distal) did not show a significant effect on any parameter. For most parameters measured, there was a significant two-way interaction between *implant surface* and *time postimplantation*, but not for the combinations of *implant surface* or *time postimplantation* with *implantation site*. The presence of these significant two-way interactions between *implant surface* and *time* showed that it was not legitimate to combine the data from different time points for subsequent data analysis. Therefore, the data from each time point were subsequently analyzed separately, using implant surface as sole variable.

3.2. Bone–implant interface

Total, surface, and within-pore BIC increased with time for all implant surfaces (Fig. 1a–c). After 3 and 6 weeks, the implants with 200-μm pores showed the highest percentage of total BIC (Fig. 1a, $P<0.05$ at 3 weeks vs. 100- and-300 μm pores). However, after 12 weeks postsurgery, total BIC did not differ between all three implants with polished surfaces, independent of pore size. The blasted 200-μm implants exhibited the highest values for total BIC compared with all other surfaces at 12 weeks postimplantation ($P<0.05$). The increase in total BIC for blasted 200-μm pores was almost entirely due to a higher surface BIC, which was

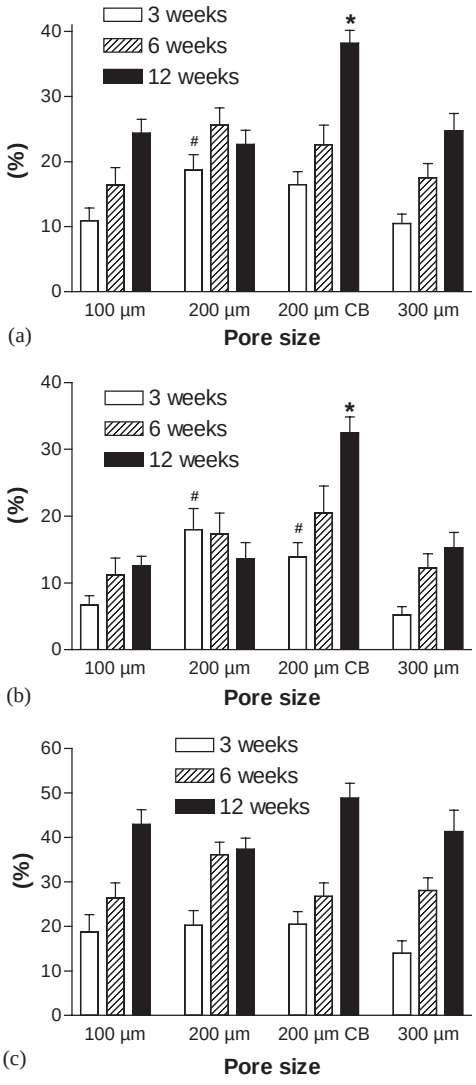

Fig. 1. Total (a), surface (b), and within-pore (c) bone–implant contact (BIC) in polished and corundum-blasted (CB), laser-textured implants at 3, 6, and 12 weeks postimplantation. Data represent mean ± SEM ($n = 11-15$ per group). $^{*}P<0.05$ vs. all other groups, $^{\#}P<0.05$ vs. 100- and 300-μm pores at the same time point by one-way ANOVA followed by Student–Newman–Keuls test.

Table 2
Three-way ANOVA analysis of selected parameters of osseointegration of polished and corundum-blasted, laser-textured implants

Parameter	Implant surface	Implantation site	Time	Two-way interactions		
				Surface/time	Surface/site	Site/time
Total BIC	$P<0.001$	NS	$P<0.001$	$P = 0.005$	NS	NS
Surface BIC	$P<0.001$	NS	$P<0.001$	$P = 0.002$	NS	NS
Within-pore BIC	NS	NS	$P<0.001$	NS	NS	NS
%Pore filling	$P<0.001$	NS	$P<0.001$	$P = 0.020$	NS	NS
%Lamellar bone	$P<0.001$	NS	$P = 0.007$	NS	NS	NS

BIC, bone–implant contact; NS, not significant; The percentage of lamellar bone was quantified within the pores of the implants.

about twice as high relative to all other implants (Figs. 1b and 2, $P<0.05$). Within-pore BIC was not influenced by pore geometry or surface blasting (Fig. 1c).

3.3. Pore filling and bone quality inside pores

Pore filling increased with time for all implant surfaces (Fig. 3a). At 6 and 12 weeks postsurgery, pore filling was lowest for the 100-μm pores (Figs. 2 and 3a, $P<0.05$). A similar trend was seen for the 3-week time point. Also, the amount of lamellar bone found within pores increased with time for all implants (Fig. 3b). Pore size was a major determinant of the percentage of within-pore lamellar bone. At all time points, implants with bigger pores showed more lamellar bone within pores, independent of surface blasting. Only very little lamellar bone was found in 100-μm pores at the end of the study period.

3.4. Bone formation within pores and in peri-implant bone

To examine the dynamics of bone growth within the pores and in peri-implant bone, we performed multiple fluorochrome labeling. Data are shown for the 6- and 12-week time point only. Generally, the bone formation rates per mm^2 pore area reached higher values in the 6-week compared with the 12-week group, showing that bone remodeling in this model was most intense 4–6 weeks postimplantation (Fig. 4a–b). In the group of animals killed at 6 weeks postimplantation, the bone

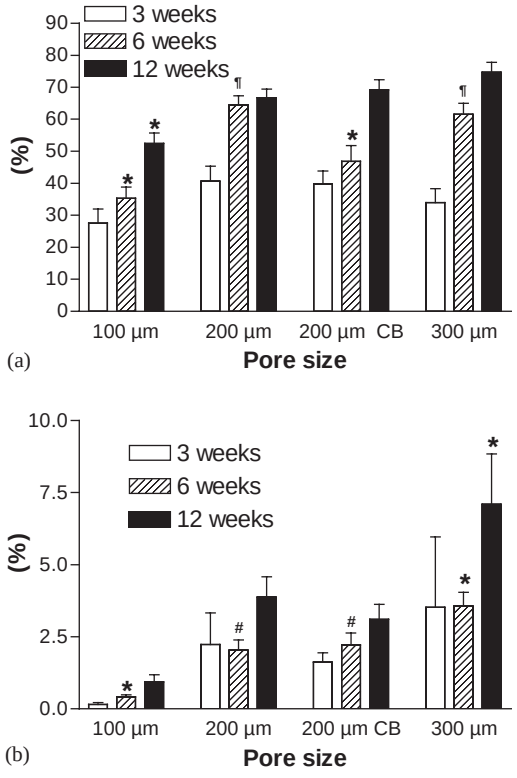

Fig. 3. Percent pore filling (a) and percent lamellar bone present within pores (b) in polished and corundum-blasted (CB), laser-textured implants at 3, 6, and 12 weeks postimplantation. Data represent mean ± SEM ($n = 11-15$ per group). * $P<0.05$ vs. all other groups, # $P<0.05$ vs. 100- and 300-μm pores, ¶ $P<0.05$ vs. 100- and 200-μm CB pores at the same time point by one-way ANOVA followed by Student–Newman–Keuls test.

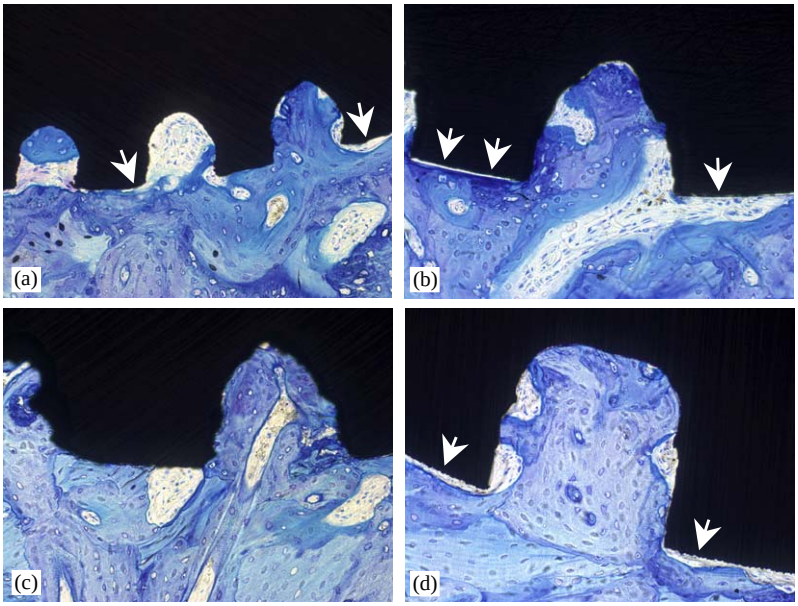

Fig. 2. Photomicrographs of laser-textured TiAlV implants with 100- (a), 200- (b), surface-blasted 200- (c), and 300-μm pores (d), 12 weeks postimplantation. Note that pore filling is lower for the 100-μm pores (a), and that bone tends to avoid the polished surfaces of the implants that were not surface blasted (a,b,d), leaving a visible gap between the implant and the surrounding bone tissue (arrows). The corundum-blasted implant with 200-μm pores (c) shows ample bone–implant contact at the inter-pore surface. It is evident that distinct fluorochrome labels indicative of lamellar bone formation are present in all pores, independent of their size (a–d). Sections were stained with toluidine blue, original magnification × 200.

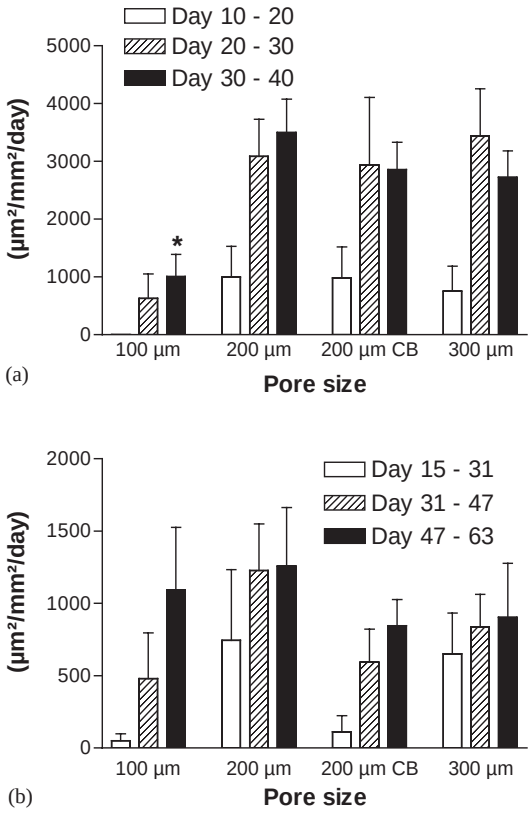

Fig. 4. Bone formation rate within pores in polished and corundum-blasted (CB), laser-textured implants at 6 (a), and 12 weeks (b) postimplantation. The bone formation rate was normalized to the pore area. Data represent mean ± SEM ($n = 11$–15 per group). *$P < 0.05$ vs. all other groups at the same time point by one-way ANOVA followed by Student–Newman–Keuls test.

formation rate in the 100-µm pores was lower compared with all other implant surfaces for the time interval between days 30 and 40 of the study (Fig. 4a). A similar trend was seen for the earlier labeling intervals (Fig. 4a). However, at the later time points, lamellar bone formation in the 100-µm pores increased, and for the time interval between days 47 and 63 of the study there were no significant differences in bone formation rates between the different surfaces any more (Fig. 4b). In peri-implant bone tissue, we did not observe any differences in bone formation rates between the different implant surfaces in the 12-week group (data not shown). In agreement with the above-mentioned measurements of lamellar/woven bone made under polarized light, fluorochrome labeling showed the presence of well-defined, linear labels also in 100-µm pores, 12 weeks postsurgery (Fig. 5a–d).

4. Discussion

In the current study, we have demonstrated that surface blasting significantly enhances the osseointegration of laser-textured Ti6Al4 V implants in a rabbit transcortical implantation model. The increased total BIC in blasted 200-µm implants was almost entirely due to increased BIC at the implant surface. Compared with polished 200-µm implants the higher surface BIC in blasted 200-µm implants was not observed at 3 weeks postimplantation, but developed mainly between 6 and 12 weeks postsurgery, suggesting that the biological

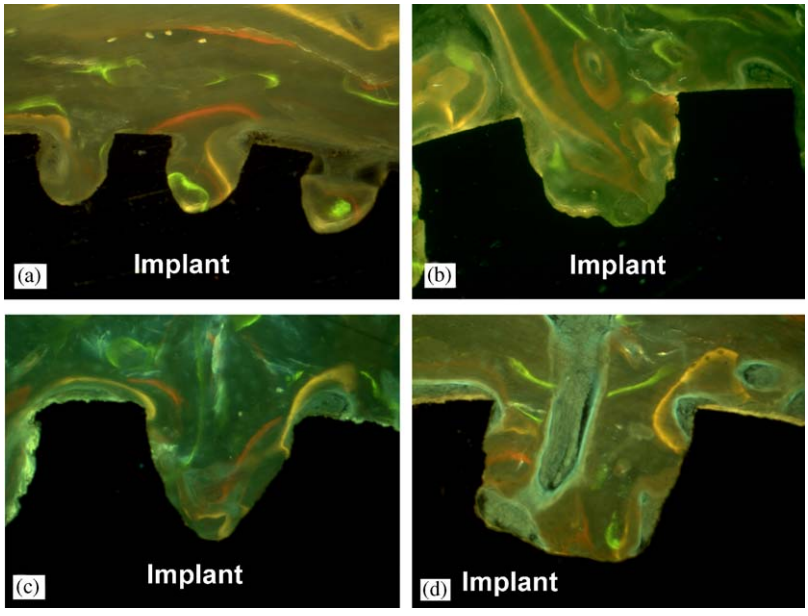

Fig. 5. Photomicrographs of laser-textured Ti6Al4 V implants with 100- (a), 200- (b), surface-blasted 200- (c), and 300-µm pores (d), viewed under epifluorescent light, 12 weeks postimplantation. The animals were labeled with four different fluorochromes according to the regimen shown in Table 1. Fluorochrome labels in bone tissue are visualized by blue–violet excitation. It is evident that distinct fluorochrome labels indicative of lamellar bone formation are present in all pores, independent of their size (a–d). Unstained sections, original magnification ×200.

mechanisms involved in bone ingrowth preferentially used the pores to initially anchor the implant within newly formed bone. At the later stages of osseointegration, bone growth spread onto the implant surface, depending on the structure of this surface. In agreement with this notion, within-pore BIC was always higher than surface BIC for all implants at all time points. Interestingly, surface blasting after the introduction of pores with defined geometry by Nd:YAG laser technique did not enhance BIC within the pores. Obviously, the local evaporation of the titanium alloy induced by the pulsed laser beam left a surface of sufficient roughness for optimal bone ingrowth within the pores.

For long-term biomechanical integrity of the bone–implant interface, remodeling of the initially formed woven bone and of microdamage [27] generated by mechanical loading is a crucial process. In our previous study [31] using a rabbit intramedullary implantation model we found lamellar bone and bone remodeling in 200-μm, but not in 25- or 50-μm pores created by laser texturing. Many years ago, Hulbert et al. [24] had demonstrated that the development of osteons requires minimum pore diameters between 150 and 200 μm in ceramic implants. In agreement with these findings, Li et al. [12] reported that laser-treated surfaces require pores of at least 140 μm diameter for osteon formation in a rabbit transcortical model. However, the present study has clearly shown that bone remodeling does occur in pores with 100 μm diameter, albeit with a pronounced time lag relative to larger pores. The delayed onset of bone remodeling in 100-μm pores may be an important argument against the use of such small pore sizes, because it can be assumed that the delayed bone remodeling within the pores is associated with decreased mechanical stability within the first weeks after implantation compared to implants with larger pores. Three-hundred-μm pores had the highest percentage of lamellar bone at the end of the study. However, the 300-μm pores were inferior to 200-μm pores in terms of total, surface, and within-pore BIC at 3 weeks postimplantation, suggesting that osseointegration of the implants with larger pores was slower. Thus, it remains to be shown in a long-term study whether the potential advantage of an improved mechanical stability due to a higher extent of bone remodeling within the pores could outweigh the initially slower osseointegration of laser-textured implants with 300-μm pores.

Laser treatment of metal implants may be a very interesting technology for the structuring of implant surfaces. Bone ingrowth into pores causes interlocking of the surrounding bone tissue with the implant, and may result in improved biomechanical stability and higher resistance to fatigue loading [20–22]. In this context, our finding that initial bone ingrowth is preferentially directed toward the pores of the implant may indicate further advantages of laser-textured implants with open pores due to an improved stability during the early stages of osseointegration. This hypothesis needs to be tested in future experiments.

Taken together, our study has clearly shown that additional surface blasting of laser-textured Ti6Al4 V implants with 200-μm pores results in a profound improvement in osseointegration, 12 weeks postimplantation. Furthermore, the available data suggest that a diameter of around 200 μm may be the optimal size of pores in laser-textured Ti6Al4 V implants. At present, larger pore sizes do not seem to offer major advantages. Clearly, more experimentation is required to demonstrate that surface-blasted, laser-textured implants are superior to standard surface-blasted implants in terms of osseointegration and mechanical stability in different models.

Acknowledgements

We would like to thank the AZT-EVUS Co., Vilseck, the P. Brehm Co., Weisendorf, and Dr. M. Hartmann from the Arges Co., Nabburg, for their assistance in providing the laser-textured implants. We also thank Prof. Dr. Thiede and Prof. Dr. Ulrichs, Department of Surgery, University of Würzburg, for their generous permission to use their animal facilities. This study was supported by a research grant from the Bavarian Ministry for Culture (High Tech Offensive Bayern).

References

[1] Schenk RK, Buser D. Osseointegration: a reality. Periodontol 2000 1998;17:22–35.
[2] Branemark PI. Osseointegration and its experimental background. J Prosthet Dent 1983;50:399–410.
[3] Szmukler-Moncler S, Salama H, Reingewirtz Y, Dubruille JH. Timing of loading and effect of micromotion on bone-dental implant interface: review of experimental literature. J Biomed Mater Res 1998;43:192–203.
[4] Spears IR, Pfleiderer M, Schneider E, Hille E, Morlock MM. The effect of interfacial parameters on cup-bone relative micromotions. A finite element investigation. J Biomech 2001;34:113–20.
[5] Donath K. Vergleichende histologische Untersuchung verschiedener enossaler Implantattypen. Z Zahnaerztl Implantol 1988;4:106–8.
[6] Davies JE. Mechanisms of endosseous integration. Int J Prosthodont 1998;11:391–401.
[7] Aspenberg P, Goodman S, Toksvig-Larsen S, Ryd L, Albrektsson T. Intermittent micromotion inhibits bone ingrowth. Titanium implants in rabbits. Acta Orthop Scand 1992;63:141–5.
[8] Gondolph-Zink B. [Effect of hydroxyapatite layering on the osteo-integration of weightbearing and non-weightbearing implants. Comparison to other microporous surfaces in animal experiments]. Orthopäde 1998;27:96–104.
[9] Brunski JB. In vivo bone response to biomechanical loading at the bone/dental-implant interface. Adv Dent Res 1999;13:99–119.

[10] Chang YS, Gu HO, Kobayashi M, Oka M. Influence of various structure treatments on histological fixation of titanium implants. J Arthroplasty 1998;13:816–25.
[11] D'Lima DD, Lemperle SM, Chen PC, Holmes RE, Colwell Jr CW. Bone response to implant surface morphology. J Arthroplasty 1998;13:928–34.
[12] Li J, Liao H, Fartash B, Hermansson L, Johnsson T. Surface-dimpled commercially pure titanium implant and bone ingrowth. Biomaterials 1997;18:691–6.
[13] Schwartz Z, Boyan BD. Underlying mechanisms at the bone-biomaterial interface. J Cell Biochem 1994;56:340–7.
[14] Kasemo B, Gold J. Implant surfaces and interface processes. Adv Dent Res 1999;13:8–20.
[15] Thomas KA, Kay JF, Cook SD, Jarcho M. The effect of surface macrotexture and hydroxylapatite coating on the mechanical strengths and histologic profiles of titanium implant materials. J Biomed Mater Res 1987;21:1395–414.
[16] Buser D, Schenk RK, Steinemann S, Fiorellini JP, Fox CH, Stich H. Influence of surface characteristics on bone integration of titanium implants. A histomorphometric study in miniature pigs. J Biomed Mater Res 1991;25:889–902.
[17] Thomas KA, Cook SD. Relationship between surface characteristics and the degree of bone–implant integration. J Biomed Mater Res 1992;26:831–3.
[18] Feighan JE, Goldberg VM, Davy D, Parr JA, Stevenson S. The influence of surface-blasting on the incorporation of titanium-alloy implants in a rabbit intramedullary model. J Bone Joint Surg Am 1995;77:1380–95.
[19] Cooper LF. A role for surface topography in creating and maintaining bone at titanium endosseous implants. J Prosthet Dent 2000;84:522–34.
[20] Hulbert SF, Cooke FW, Klawitter JJ, Leonard RB, Sauer BW, Moyle DD, Skinner HB. Attachment of prostheses to the musculoskeletal system by tissue ingrowth and mechanical interlocking. J Biomed Mater Res 1973;7:1–23.
[21] Sauer BW, Weinstein AM, Klawitter JJ, Hulbert SF, Leonard RB, Bagwell JG. The role of porous polymeric materials in prosthesis attachment. J Biomed Mater Res 1974;8:145–53.
[22] Roderic L. Composite biomaterials. In: Bronzino JD, editor. The biomedical engineering handbook. Boca Raton, FL: CRC Press; 1995. p. 309–14.
[23] Bobyn JD, Pilliar RM, Cameron HU, Weatherly GC. The optimum pore size for the fixation of porous-surfaced metal implants by the ingrowth of bone. Clin Orthop 1980;150:263–70.
[24] Hulbert SF, Young FA, Mathews RS, Klawitter JJ, Talbert CD, Stelling FH. Potential of ceramic materials as permanently implantable skeletal prostheses. J Biomed Mater Res 1970;4:433–56.
[25] Klawitter JJ, Weinstein AM. The status of porous materials to obtain direct skeletal attachment by tissue ingrowth. Acta Orthop Belg 1974;40:755–65.
[26] Parfitt AM. Osteonal and hemi-osteonal remodeling: the spatial and temporal framework for signal traffic in adult human bone. J Cell Biochem 1994;55:273–86.
[27] Frost HM. Some ABC's of skeletal pathophysiology. 5. Microdamage physiology. Calcif Tissue Int 1991;49:229–31.
[28] Mittelmeier W, Grunwald I, Schafer R, Grundei H, Gradinger R. [Cementless fixation of the endoprosthesis using trabecular, 3-dimensional interconnected surface structures]. Orthopade 1997;26:117–24.
[29] Lacefield WR. Materials characteristics of uncoated/ceramic-coated implant materials. Adv Dent Res 1999;13:21–6.
[30] Bergmann HW, Hartmann M. Drilling of metals with copper vapour lasers. In: Mazumder J, Mukherjee K, editors. Laser materials processing IV. Warrendale, PA: The Minerals, Metals & Materials Society; 1994. p. 33–44.
[31] Stangl R, Pries A, Loos B, Müller M, Erben RG. Influence of pores created by laser superfinishing on osseointegration of titanium alloy implants. J Biomed Mater Res, submitted for publication.
[32] Schenk RK, Olah AJ, Herrmann W. Preparation of calcified tissues for light microscopy. In: Dickson GR, editor. Methods of calcified tissue preparation. Amsterdam: Elsevier; 1984. p. 1–56.
[33] Donath K, Breuner G. A method for the study of undecalcified bones and teeth with attached soft tissues. The Sage-Schliff (sawing and grinding) technique. J Oral Pathol 1982;11:318–26.